مجلة المنتدى الأكاديمي (العلوم التطبيقية)
المجلد (9) العدد (1) 2025
ISSN (Print): 2710-446x , ISSN (Online): 2710-4478
تاريخ التقديم: 2025/02/02 ، تاريخ القبول: 2025/03/13، تاريخ النشر: 2025/03/17

Sustainable energy future for Libya: Assessing the solar energy potential of twenty-three urban areas

Jumaa F. Alnaas [1], Abduslam Sharif [1], Mohamed S. Altraiki[2]

[1]Chemical and Petroleum Engineering Department, Faculty of Engineering Al Khums, Elmergib University, Libya
E-mail: alnaasjumaa@gmail.com, a6sharif@uwaterloo.ca
[2] Libyan Center for Sustainable Development Research, Libyan Authority for Scientific Research, Libya
E-mail: mstraiki@lsd.ly

Abstract

Libya's solar energy potential is vast and largely untapped. By strategically harnessing this resource, Libya can move towards a sustainable energy future that reduces its dependence on fossil fuels, lowers carbon emissions, and promotes economic growth. This study assesses Libya's solar energy potential by analyzing solar radiation data from twenty-three cities across the country using data from the NASA database. This study suggests that Libya is highly suited for solar energy, with various regions showing estimated solar radiation values ranging from 1,936 $kWh\cdot m^{-2}$ for Khums to 2,459 $kWh\cdot m^{-2}$ per year for Al-Kufrah. Southern regions, particularly Al-Kufrah 24,256,829 $J\cdot m^{-2}\cdot day^{-1}$, Marzuq 24,128,866 $J\cdot m^{-2}\cdot day^{-1}$, and Gat 22,698,253 $J\cdot m^{-2}\cdot day^{-1}$, exhibit the highest solar radiation levels, making them prime candidates for large-scale solar projects. In contrast, northern cities such as Khums 19,097,772 $J\cdot m^{-2}\cdot day^{-1}$, Al-Bayda 19,327,052 $J\cdot m^{-2}\cdot day^{-1}$, and Tripoli 19,547,572 $J\cdot m^{-2}\cdot day^{-1}$ show comparatively lower solar radiation, indicating reduced feasibility for solar installations. Seasonal variations, especially during summer, show peak solar energy potential, emphasizing the need for strategic planning and potential incorporation of energy storage solutions. The study's findings align with regional solar radiation trends observed in similar climates, validating the model's accuracy. This study provides critical insights for policymakers and investors, supporting Libya's transition towards renewable energy and contributing to its sustainability goals.

Keywords: - Solar energy, Solar radiation, Renewable energy, Libya

1. Introduction

1.1 Importance of solar energy as a renewable and sustainable

The growing concern over the environmental impacts of fossil fuels has driven the shift towards green energy, particularly focusing on renewable energy sources for electricity generation. Governments and companies worldwide are prioritizing the reduction of greenhouse gas emissions by adopting sustainable energy alternatives. Solar power, due to its numerous advantages, is considered the most favorable option among renewable energy resources (Strielkowski et al., 2021). In comparison to a nuclear power plant, which converts 0.130 kg of nuclear fuel into 1,000 MW of electricity annually, the sun converts approximately 4 million tons of solar fuel into energy every second (Majeed et al., 2023).

From 2010 to 2021, the global number of people lacking access to electricity decreased from 1.14 billion to 675 million. Because Africa's population is continuously increasing, there was only a small drop in its population without access to electricity, decreasing from 591 million to 586 million during that time. The 2023 *Tracking SDG7 Report* forecasts that 660 million individuals, primarily located in Sub-Saharan Africa, will continue to lack access by the year 2030. The goal of United Nations Sustainable Development Goal (SDG) 7 is to ensure accessible, reliable, and clean energy for all by 2030, addressing the worldwide energy disparity. (Ritchie et al., 2024)

The global community recognizes that access to electricity is a crucial initial move towards reaching socioeconomic progress. Nonetheless, approximately 1 billion individuals across the globe lack electricity access, leading to a limited potential to enhance their standard of living. The majority of the population is poor and lives in rural areas where it would be costly to extend the electrical grid.(Yadav et al., 2019)

1.2 Geographic profile and energy status of Libya

Libya, located in North Africa between latitudes 19° and 34°N and longitudes 9° and 25°E, covers an area of approximately 1.76 million square kilometers, making it the fourth-largest country in Africa Over 90% of the nation is covered in semi-desert or desert terrains. Therefore, there are approximately 3,000 to 4,000 hours of sunlight annually making the country among the highest levels of solar radiation globally (Mohamed & Masood, 2018). Libya possessed 39% of Africa's proven oil reserves and 3% of the worlds proved oil reserves as of the end of 2021 which equal to 48.36 billion barrels (Matori, 2024).

Following 2011, however, GECOL experienced a loss of certain infrastructure assets, a deterioration in the operation of the power network, and ultimately, a severe shortage of power-generating capacity. This resulted in extended power outages in numerous regions of the nation, particularly during the summer and winter peak load periods. These events were caused by insecurity and political instability. Furthermore, the ongoing shift in power generation from oil to gas has been problematic despite being well-justified from an economic and environmental standpoint. This is because the infrastructure for gas pipelines and the production of natural gas have not kept up with demand, forcing some plants to run on fuel oil.(Irhiam et al., 2023)

The extensive review of GECOL by the Libyan Audit Bureau has resulted in recent media reports verifying that capacity shortages have continued into 2021, as the available generating capacity of 5 to 5.5 GW remains insufficient to meet the winter demand of 7 GW and the summer demand of 8 GW. Since around 2016, Libya has maintained a total electricity generation capacity of approximately 10 to 11 GW according to the EIA 2020. The actual available capacity is significantly lower than the stated nominal or nameplate capacities.(Almaktar & Shaaban, 2021)

In Libya, most of the energy is generated from gas and oil, while the use of renewable resources for energy production is nearly non-existent. Because Libya has plenty of fossil fuel resources, the focus on developing alternative energy has been limited so far. The majority of the country's revenue comes from oil and gas, which puts further pressure on its natural resources. If the nation continues on its current path, it may end up overlooking its sustainable development goals. Decision-makers are likely to find the sustainability research to be of interest. As a result, the Libyan government formed the Libyan Renewable Energy Authority (REAOL) in 2007 to reach the target of having 10% of the nation's energy combination sourced from renewable sources by 2020.(Yahya et al., 2020)

As the purpose of evaluating solar energy potential at a specific location is to ascertain the practicality and feasibility of constructing solar power systems, estimating solar radiation is crucial for data and analysis of solar potentials in a given area. The potential solar energy for each of the twenty-three Libyan cities is evaluated based on the meteorological data presented in Table 1. The selection of these cities was predicated upon the accessibility and availability of solar radiation data. The techniques utilized to create and gather these data are described in depth in NASA climatological data for renewable energy assessment (Chandler et al., 2004).

2. Model description

2.1 Solar declination

Solar declination is the angle between the rays of the sun and the plane of the Earth's equator. The angle ranges from zero in fall and spring to a maximum of 23½° in summer and -23½° in winter (Eicker, 2003). The daily solar declination (δ) in degrees is given by (Cooper, 1969):

$$\delta = 23.45 \times \sin\left[\frac{360}{365}(284 + n)\right] \qquad (1)$$

Where n is the day of the year from 1 to 365. February is counted as having 28 days. The monthly average solar declination ($\overline{\delta}$) in degrees, where $\overline{n}$ is the mid of the month in days, is given by:

$$\overline{\delta} = 23.45 \times \sin\left[\frac{360}{365}(284 + \overline{n})\right] \qquad (2)$$

2.2 Sunrise hour angle

The sunrise hour angle is the negative of the sunset hour angle. The daily sunrise hour angle (ω_s) in degrees is given by:

$$\omega_s = \cos^{-1}[-\tan\phi \cdot \tan\delta] \qquad (3)$$

Where ϕ is the geographic latitude in degrees; north positive and south negative. The monthly average daily sunrise hour angle ($\overline{\omega}_s$) in degrees is given by:

$$\overline{\omega}_s = \cos^{-1}\left[-\tan\phi \cdot \tan\overline{\delta}\right] \qquad (4)$$

The daily sunrise hour angle for a tilted surface facing the equator (ω_s') in degrees is given by:

$$\omega_s' = \cos^{-1}[-\tan\delta\ \tan(\phi-\beta)] \qquad (5)$$

Where (β) is the inclination slope in degrees from the horizontal position. In the summer in northern hemisphere $\delta > 0$, and this results in $\omega_s > \omega_s'$, and in the winter in northern hemisphere $\delta < 0$ and this results in $\omega_s < \omega_s'$. The sunrise hour angle for the tilted surface for the mean day of the month ($\overline{\omega}_s'$) in degrees is given by (Iqbal, 2012):

$$\overline{\omega}_s' = \min\left\{\cos^{-1}\left[-\tan\phi \cdot \tan\overline{\delta}\right], \cos^{-1}\left[-\tan\overline{\delta}\ \tan(\phi-\beta)\right]\right\} \qquad (6)$$

2.3 Number of daylight hours

The number of daylight hours depends on the geographic location and time of the year. More daylight hours mean more energy can be harnessed, improved efficiency, and higher revenue potential. The day length is $2\omega_s$. So, the daily number of daylight hours (N) is given by:

$$N = \frac{2}{15}\cos^{-1}(-\tan\phi \cdot \tan\delta) \qquad (7)$$

The monthly average daily number of daylight hours ($\overline{N}$) is given by:

$$\overline{N} = \frac{2}{15}\cos^{-1}\left(-\tan\phi \cdot \tan\overline{\delta}\right) \qquad (8)$$

2.4 Eccentricity correction factor

The eccentricity correction factor is used to account for the variations in solar radiation intensity brought on by the varying Earth-Sun distance. Taking the eccentricity correction factor in solar energy evaluation into consideration improves the accuracy and performance of energy models. The daily eccentricity correction factor, *f*, is calculated from very simple expression used by (Duffie & Beckman, 1980):

$$f = 1 + 0.033\cos\left(\frac{360}{365}n\right) \qquad (9)$$

Because solar radiations vary significantly from day to day, the monthly average daily eccentricity correction factor helps in smoothing out these variations offering improved energy prediction, more accurate models, and enhanced solar system design. The monthly average daily eccentricity correction factor, $\overline{f}$, is given by (Duffie & Beckman, 1980):

$$\overline{f} = 1 + 0.033 \cos\left(\frac{360}{365}\overline{n}\right) \tag{10}$$

2.5 Global radiation

The estimation of the monthly average daily global radiation refers to the calculation of the amount of solar radiation reaches the Earth's surface on a daily basis, averaged over a month. This data is crucial for designing and optimizing solar energy systems as it helps to determine the potential energy generation capacity of solar panel in a specific location. The monthly average daily global radiation is taken from NASA(Atmospheric Science Data Center. [Accessed June 20th, 2020).

2.6 Extraterrestrial radiation on a horizontal surface

The extraterrestrial daily radiation on horizontal surfaces refers to the amount of solar radiation that would reach the Earth's surface under clear sky conditions without any atmosphere, or other obstructions. It is a theoretical measure of the maximum amount of solar energy available at specific location. The monthly average extraterrestrial daily insolation on horizontal surfaces provides valuable information about the amount of solar energy that can potentially reach the Earth's surface during a specific month (Duffie & Beckman, 1980). The integrated daily extraterrestrial radiation on a horizontal surface from sunrise to sunset (H_0) in J·m^{-2}·day^{-1} is given by (Duffie & Beckman, 1980):

$$H_0 = \frac{24 \times 3{,}600}{\pi} G_{sc} f \left[\cos\phi \cdot \cos\delta \cdot \sin\omega_s + \frac{2\pi\omega_s}{360} \sin\phi \cdot \sin\delta\right] \tag{11}$$

Where; G_{sc}: is the solar constant, 1367 W·m^{-2} and f: is the daily eccentricity correction factor. The monthly average daily extraterrestrial radiation on a horizontal surface shows how much sun energy a place receives on average each day. It is the baseline for solar energy calculations and resource assessment. The monthly average daily extraterrestrial radiation on a horizontal surface, $\overline{H}_0$, in J·m^{-2}·day^{-1}is given by (Duffie & Beckman, 1980):

$$\overline{H}_0 = \frac{24 \times 3{,}600}{\pi} G_{sc} \overline{f} \left[\cos\phi \cdot \cos\overline{\delta} \cdot \sin\overline{\omega}_s + \frac{2\pi\overline{\omega}_s}{360} \sin\phi \cdot \sin\overline{\delta}\right] \tag{12}$$

2.7 Clearness index

Clearness index is the ratio of the average daily global radiation received at a location to the average daily extraterrestrial radiation on a horizontal surface under clear sky condition and is given by (Liu & Jordan, 1960):

$$K_t = H/H_0 \tag{13}$$

Where H is the integrated daily solar radiation on a horizontal surface, J·m^{-2}·day^{-1}. The monthly average clearness index provides valuable information about the atmospheric conditions and the amount of direct solar radiation that reaches the Earth surface. The monthly average clearness index is used to assess the quality and quantity of solar radiation available for solar energy generation. A higher value of $\overline{K}_t$ indicates clearer skies and more direct sunlight reaching the Earth's surface, while a lower value indicates cloudier conditions and reduced solar radiation intensity (Liu & Jordan, 1960). The monthly-average daily clearness index, $\overline{K}_t$, can be estimated from:

$$\overline{K}_t = \overline{H}/\overline{H}_0 \tag{14}$$

Insolation-sunshine correlations are valid only for long-term averages and can estimated by (Prescott, 1940):

$$\frac{\overline{H}}{\overline{H}_0} = a + b\frac{\overline{n}}{\overline{N}} \tag{15}$$

Where; a, b: Constants depend on location; $\overline{N}$: The monthly average day length, *i.e.*, day length of the average day of the month.

2.8 Daily diffuse

The amount of solar energy that reaches the Earth's surface after being scattered by the atmosphere is referred to as daily diffuse radiation. It provides information on the amount of scattered sunlight that contributes to the total solar radiation received at specific location. This parameter is important for understanding the distribution of solar energy throughout the day and its impact on the performance of solar energy system. The daily diffuse, H_d, in J·m^{-2}·day^{-1} can be estimated based on the value of the daily sunset hour angle and the daily clearness index. If $\omega_s \leq 81.4°$, then (Erbs et al., 1982):

$$H_d = H \times \begin{cases} 1.0 - 0.2727K_T + 2.4495K_T^2 - 11.9514K_T^3 + 9.3879K_T^4 & \text{for } K_T < 0.715 \\ 0.143 & \text{for } K_T \geq 0.715 \end{cases} \tag{16}$$

If $\omega_s > 81.4°$, then:

$$H_d = H \times \begin{cases} 1.0 + 0.2832K_T - 2.5557K_T^2 + 0.8448K_T^3 & \text{for } K_T < 0.722 \\ 0.175 & \text{for } K_T \geq 0.722 \end{cases} \tag{17}$$

This parameter is important for understanding the distribution of solar energy throughout the day and its impact on the performance of solar energy system. The monthly average daily diffuse radiation can be estimated based on the value of the monthly average daily sunset hour angle and the monthly average clearness index as follows (Erbs et al., 1982):

If $\omega_s \leq 81.4°$ and $0.3 \leq \overline{K}_t \leq 0.8$, then:

$$\overline{H}_d = \overline{H} \cdot \left(1.391 - 3.560\overline{K}_t + 4.189\overline{K}_t^2 - 2.137\overline{K}_t^3\right) \tag{18}$$

If $\omega_s > 81.4°$ and $0.3 \leq \overline{K}_t \leq 0.8$, then:

$$\overline{H}_d = \overline{H} \cdot \left(1.311 - 3.022\overline{K}_T + 3.427\overline{K}_T^2 - 1.821\overline{K}_T^3\right) \qquad (19)$$

2.9 Daily beam radiation on a horizontal surface

Beam radiation refers to the direct solar radiation that reaches a surface without any scattering or diffusion. This type of radiation comes directly from the sun in a straight line and is a key component of the total solar radiation received at a specific location. The daily beam, direct, radiation on horizontal surface in J·m^{-2}·day^{-1} can be calculated from:

$$H_b = H - H_d \qquad (20)$$

This parameter is significant for understanding the availability of direct solar radiation and optimizing the performance of solar energy systems. Analyzing the monthly average daily beam radiation on a horizontal surface can help solar energy designer assess the solar resource potential, optimize the position, and predict energy generation from solar installations. The monthly average daily beam, direct, radiation on a horizontal surface:

$$\overline{H}_b = \overline{H} - \overline{H}_d \qquad (21)$$

2.10 Ratio of the monthly average daily beam radiation on a tilted to that on a horizontal surface

The ratio, $\bar{R}_b$, of the monthly average daily beam radiation on a tilted surface, $\overline{H}_{bt}$, to that on a horizontal surface, $\overline{H}_b$, for each month in the absence of the Earth's atmosphere is given by (Liu & Jordan, 1960):

$$\bar{R}_b = \overline{H}_{bt}/\overline{H}_b \qquad (2)$$

or,

$$\bar{R}_b = \frac{\cos(\phi - \beta)\cos\delta\sin\omega_s' + \frac{\pi}{180}\omega_s'\sin(\phi - \beta)\sin\delta}{\cos\phi\cos\delta\sin\omega_s + \frac{\pi}{180}\omega_s\sin\phi\sin\delta} \qquad (3)$$

The ratio of the daily average radiation on a tilted surface to that on a horizontal surface for each month assuming isotropic conditions [16]:

$$\bar{R} = \bar{R}_b\left(1 - \frac{\overline{H}_d}{\overline{H}}\right) + \frac{1}{2}\frac{\overline{H}_d}{\overline{H}}(1 + \cos\beta) + \frac{\bar{\rho}_g}{2}(1 - \cos\beta) \qquad (4)$$

Where $\bar{\rho}_g$ is the reflectivity of the ground or albedo. Albedo is the fraction of sunlight that is reflected by the Earth's surface. Despite the many factors affecting albedo including the presence of clouds, aerosols, type of the surface among others, albedo known to change very little over time. The global annual mean value is 29% which is equivalent to 99.7 W·m^{-2} (Stephens et al., 2015).

2.11 Solar radiation on tilted surface

The daily solar radiation on tilted surface in J·m^{-2}·day^{-1} can be expressed as (Stephens et al., 2015):

$$H_t = H_b \bar{R}_b + \frac{H_d}{2}(1+\cos\beta) + \frac{H\rho_g}{2}(1-\cos\beta) \qquad (5)$$

The monthly average solar radiation on tilted surface in J·m^{-2}·day^{-1} can be expressed as (Stephens et al., 2015):

$$\bar{H}_t = \bar{H}_b \bar{R}_b + \frac{\bar{H}_d}{2}(1+\cos\beta) + \frac{\bar{H}\bar{\rho}_g}{2}(1-\cos\beta) \qquad (6)$$

Table 1. Geographical characteristics and average air temperature for some Libyan cities(Atmospheric Science Data Center. [Accessed June 20th, 2020).

No.	Location	Latitude	Longitude	Elevation	Average air temperature
		Degrees	Degrees	m	°C
1	Agedabia	30.72	20.17	7	20.8
2	Al-Bayda	32.76	21.62	345	20.2
3	Al-Burayqah	30.39	19.61	8	22.7
4	Al-Kufrah	24.20	23.29	413	22.8
5	Awbari	26.58	12.77	586	22.8
6	Awjilah	29.11	21.29	27	23.1
7	Bani Walid	31.77	13.99	436	20.7
8	Benghazi	32.10	20.27	132	20.0
9	Darnah	32.77	22.64	238	20.4
10	Gadamis	30.15	9.50	360	22.0
11	Gat	24.97	10.17	978	22.0
12	Hun	29.12	15.94	352	21.9
13	Khums	32.66	14.26	71	20.9
14	Marzuq	25.93	13.91	622	22.6
15	Misurata	32.42	15.05	32	20.4
16	Mizdah	31.43	12.98	604	20.1
17	Nalut	31.88	10.97	450	21.2
18	Sabha	27.07	14.42	434	22.4
19	Sirte	31.20	16.58	14	20.7
20	Suluq	31.67	20.25	117	21.9
21	Tripoli	32.70	13.08	63	20.5
22	Tubruq	32.08	23.96	23	20.6
23	Waddan	29.17	16.13	387	22.1

3. Results and analysis

3.1 Average monthly temperature

The average monthly temperatures typically fluctuate throughout the year, reflecting the changing seasons. Different locations exhibit varying average monthly maximum temperatures due to factors such as latitude, elevation, and local geography. Coastal areas often have milder temperatures compared to inland areas, which may experience more extreme temperatures. Figures 1, 2, and 3 show the average monthly temperature for the selected cities. These data, as explained earlier, are based on NASA recordings from January 2005 to December 2014.

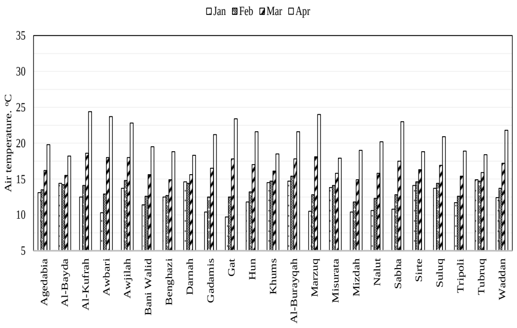

Figure 1. Average monthly temperature (Jan – Apr).

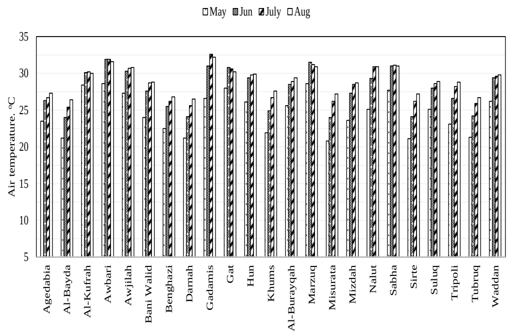

Figure 2. Average monthly temperature (May – Aug).

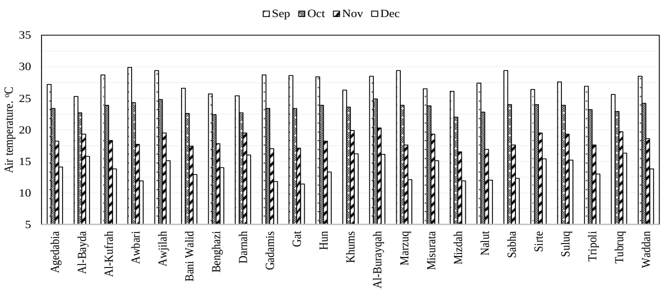

Figure 3. Average monthly temperature (Sep – Dec)

The average air temperature ranges from a minimum of 9.7 ^{o}C in January for Gat to a maximum of 32.6 ^{o}C in July for Gadamis. The annual average temperature ranges from a minimum of 20 ^{o}C in Benghazi to a maximum of 23.1 ^{o}C in Awjilah.

3.2 Estimation of the monthly average daily sunrise hour angle for a tilted surface

In January, the angle is estimated to range from 75.5^{o} to 79.9^{o}. While in February, the sunrise hour angle ranges from 80.6^{o} to 83.4^{o}. By March and April, the sunrise hour angle continues to increase with values ranging from 88.2^{o} to 88.7^{o} in March, and 90^{o} in April which is relatively consistent across the locations. The angle is 90^{o} for the months of May, June, July, and August. The angle is almost the same in all cities. For the months of September, October, November, and December the maximum values are 90^{o}, 85.6^{o}, 81.1^{o}, and 78.8^{o} respectively; while the minimum values are 90^{o}, 83.7^{o}, 77.3^{o}, and 73.9^{o} respectively.

3.3 Estimation of the monthly average daily global radiation

Figure 4 illustrates the variation in global radiation level across different locations from January to April. For example, Tripoli received a monthly average daily global radiation of 10,440,000 $J \cdot m^{-2} \cdot day^{-1}$ in January, which increased to 21,600,000 $J \cdot m^{-2} \cdot day^{-1}$ in April. In May the global radiation continues to increase with a maximum value of 28,008,000 $J \cdot m^{-2} \cdot day^{-1}$ in Al-Kufrah and a minimum value of 22,320,000 $J \cdot m^{-2} \cdot day^{-1}$ in Sirte. In June, the maximum value is 29,772,000 J·m^{-2}·day^{-1} in Al-Kufrah and a minimum value of 24,840,000 J·m^{-2}·day^{-1} in Sirte. In July and August, the maximum value reaches 29,376,000 J·m^{-2}·day^{-1} in Awjilah and 27,612,000 J·m^{-2}·day^{-1} in Marzuq respectively as shown in Figure 5. For the months of September, October, November, and December the maximum recorded values are 24,840,000 J·m^{-2}·day^{-1}, 21,276,000 J·m^{-2}·day^{-1}, 16,956,000 J·m^{-2}·day^{-1} and 14,220,000 J·m^{-2}·day^{-1}, for the cities of Al-Kufrah, Al-Kufrah, Al-Kufrah and Gat respectively as shown in Figure 6. The top five cities in annual average global radiation are Al-Kufrah (22,926,000 J·m^{-2}·day^{-1}), Marzuq (22,563,000 J·m^{-2}·day^{-1}), Gat (21,249,000 J·m^{-2}·day^{-1}), Awbari (21,243,000 J·m^{-2}·day^{-1}), and Awjilah (20,826,000 J·m^{-2}·day^{-1}). The cities with the least annual global radiation are Khums (17,706,000 J·m^{-2}·day^{-1}), Tripoli (17,970,000 J·m^{-2}·day^{-1}), Al-Bayda (18,069,000 J·m^{-2}·day^{-1}), Sirte (18,120,000 J·m^{-2}·day^{-1}), and Agedabia (18,468,000 J·m^{-2}·day^{-1}).

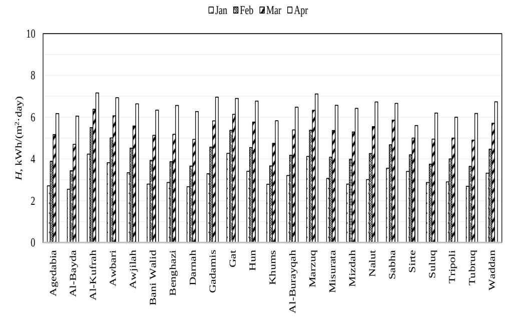

Figure 4. Monthly average daily global radiation (Jan – Apr).

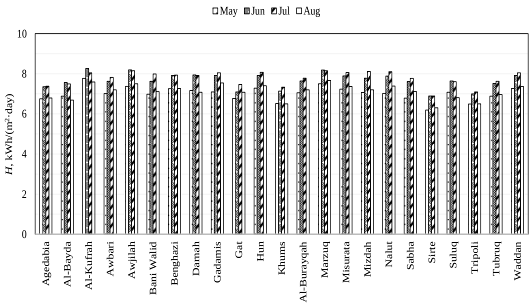

Figure 5. Monthly average daily global radiatic (May – Aug).

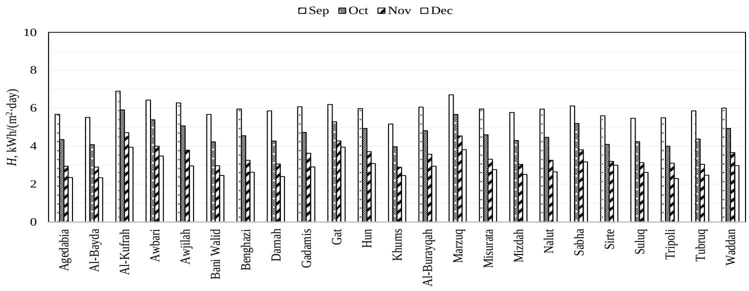

Figure 6. Monthly average daily global radiation (Sep – Dec).

3.4 Estimation of the monthly average extraterrestrial daily insolation on horizontal surfaces

The monthly average extraterrestrial daily insolation on horizontal surfaces data is important for understanding the seasonal variations in solar radiation and for assessing the solar energy potential of particular locations. The maximum values for the months of January, February, March, and April are estimated to be 24,419,394 J·m^{-2}·day^{-1}, 28,153,897 J·m^{-2}·day^{-1}, 33,387,016 J·m^{-2}·day^{-1}, and 37,485,652 J·m^{-2}·day^{-1}, respectively, all in Al-Kufrah. The minimum values are 19,392,885 J·m^{-2}·day^{-1}, 23,734,429 J·m^{-2}·day^{-1}, 30,307,416 J·m^{-2}·day^{-}

^{1}, 36,145,818 $J{\cdot}m^{-2}{\cdot}day^{-1}$, respectively, all in Darnah. In locations such as Agedabia, Al-Bayda, Al-Kufrah, and others, the values increase gradually across the four months. For the months of May, June, July, and August, the maximum values are estimated to be 40,024,672 $J{\cdot}m^{-2}{\cdot}day^{-1}$, 41,439,021 $J{\cdot}m^{-2}{\cdot}day^{-1}$, 40,733,546 $J{\cdot}m^{-2}{\cdot}day^{-1}$, and 38,340,052 $J{\cdot}m^{-2}{\cdot}day^{-1}$ for the cities of Nalut, Darnah, Darnah, and Al-Kufrah, respectively. The months of September, October, November, and December show a decrease in the maximum values of the extraterrestrial insolation. The maximum values are 35,036,780 $J{\cdot}m^{-2}{\cdot}day^{-1}$, 30,111,447 $J{\cdot}m^{-2}{\cdot}day^{-1}$, 25,548,361 $J{\cdot}m^{-2}{\cdot}day^{-1}$, and 23,205,346 $J{\cdot}m^{-2}{\cdot}day^{-1}$ respectively all for the city of Al-Kufrah. Overall, the data provides insights into the variation in extraterrestrial daily insolation levels across different locations over the course of twelve months. The top five cities with the highest annual extraterrestrial insolation are Al-Kufrah (32,975,989 $J{\cdot}m^{-2}{\cdot}day^{-1}$), Gat (32,788,497 $J{\cdot}m^{-2}{\cdot}day^{-1}$), Marzuq (32,547,562 $J{\cdot}m^{-2}{\cdot}day^{-1}$), Awbari (32,379,951 $J{\cdot}m^{-2}{\cdot}day^{-1}$), and Sabha (32,251,230 $J{\cdot}m^{-2}{\cdot}day^{-1}$). The five cities with the lowest annual extraterrestrial insolation are Darnah (30,609,436 $J{\cdot}m^{-2}{\cdot}day^{-1}$), Al-Bayda (30,612,542 $J{\cdot}m^{-2}{\cdot}day^{-1}$), Tripoli (30,631,157 $J{\cdot}m^{-2}{\cdot}day^{-1}$), Khums (30,643,552 $J{\cdot}m^{-2}{\cdot}day^{-1}$), and Misurata (30,717,666 $J{\cdot}m^{-2}{\cdot}day^{-1}$)

3.5 Estimation of the monthly average clearness index

The monthly average clearness index estimations show a general trend of increasing values from January to June, reaching a high peak in July, and falling back from August to December as the months progress towards winter. Based on the provided data, the clearness index values vary across different locations, indicating differences in solar radiation intensity and atmospheric conditions. Some locations, such as, Al-Kufrah (0.689), Marzuq (0.688), Awbari (0.650), Gat (0.647), and Awjilah (0.645), consistently show higher annual clearness index values, suggesting clearer skies and greater solar radiation receipt. Other locations, such as Khums (0.566), Al-Bayda (0.572), Agedabia (0.575), Tripoli (0.577), and Sirte (0.581), have relatively lower annual clearness index values, indicating potentially cloudier conditions and reduced solar radiation levels. This variability in clearness index values among locations highlights the importance of site-specific assessments for solar energy projects.

3.6 Estimation of the monthly average daily diffuse radiation on a horizontal surface

Figures 7, 8, and 9 show the monthly average daily diffuse radiation on a horizontal surface from January to December. Some locations exhibit relatively stable diffuse radiation levels throughout the months, while others show more fluctuations, suggesting variation in weather conditions and solar radiation distribution. Certain locations, such as Sirte (6,231,494 $J{\cdot}m^{-2}{\cdot}day^{-1}$), Agedabia (6,166,264 $J{\cdot}m^{-2}{\cdot}day^{-1}$), Khums (6,154,019 $J{\cdot}m^{-2}{\cdot}day^{-1}$), Gat (6,142,531 $J{\cdot}m^{-2}{\cdot}day^{-1}$), and Sabha (6,119,364 $J{\cdot}m^{-2}{\cdot}day^{-1}$), consistently receive high level of diffuse radiation, indicating potentially clearer skies and significant scattering of sunlight. Other locations, such as Marzuq (5,617,609 $J{\cdot}m^{-2}{\cdot}day^{-1}$), Al-Kufrah (5,657,233 $J{\cdot}m^{-2}{\cdot}day^{-1}$), Misurata (5,686,900 $J{\cdot}m^{-2}{\cdot}day^{-1}$), Nalut (5,725,355 $J{\cdot}m^{-2}{\cdot}day^{-1}$), and Gadamis (5,775,341 $J{\cdot}m^{-2}{\cdot}day^{-1}$), show lower diffuse radiation levels during specific months, pointing towards less scattering of sunlight and potentially cloudier conditions or high polluted with particles or gases.

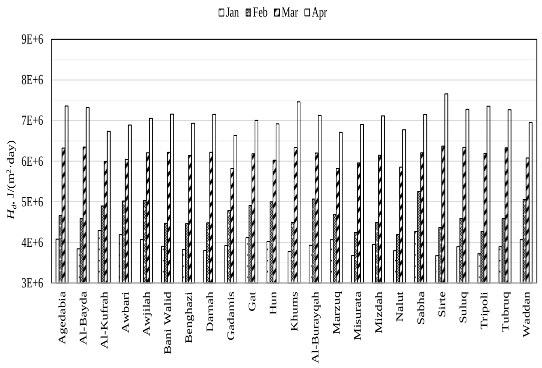

Figure 7. Monthly average daily diffuse radiation on a horizontal surface (Jan – Apr).

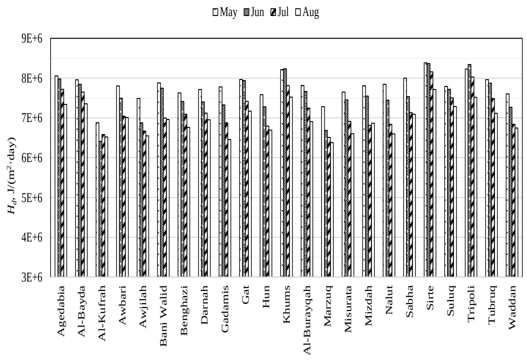

Figure 8. Monthly average daily diffuse radiation on a horizontal surface (May – Aug)

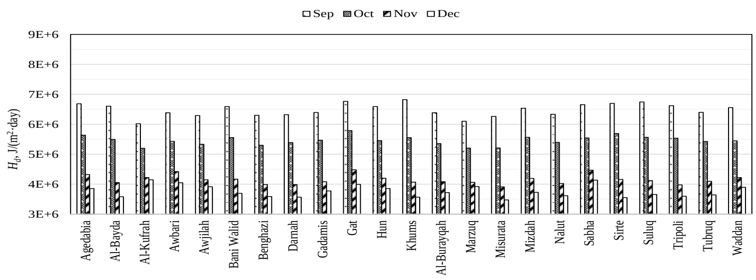

Figure 9. Monthly average daily diffuse radiation on a horizontal surface (Sep – Dec).

3.7 Estimation of the monthly average daily beam (direct) radiation on a horizontal surface

The data in Figures 10, 11, and 12 present the monthly average daily beam radiation on a horizontal surface for various locations in Libya for the months from January to December. Beam radiation levels tend to increase from January to June in many locations, as the sun's angle and intensity change with the shifting seasons, resulting in higher direct solar radiation on horizontal surfaces. The beam radiation reaches the peak in July in most cities where the maximum value is evaluated for Marzuq (22,865,519 $J \cdot m^{-2} \cdot day^{-1}$) and the minimum value is in Sirte (16,681,601 $J \cdot m^{-2} \cdot day^{-1}$). The months from August to December show a declination in the beam radiation. In general, some locations, such as Khums (11,551,981 $J \cdot m^{-2} \cdot day^{-1}$), Tripoli (11,854,987 $J \cdot m^{-2} \cdot day^{-1}$), Sirte (11,888,506 $J \cdot m^{-2} \cdot day^{-1}$), Al-Bayda (12,017,546 $J \cdot m^{-2} \cdot day^{-1}$), and Agedabia (12,300,191 $J \cdot m^{-2} \cdot day^{-1}$), show low annular beam radiation levels, indicating potential cloud cover, shading, or atmospheric interference with direct sunlight. Other locations such as Al-Kufrah (17,268,767 $J \cdot m^{-2} \cdot day^{-1}$), Marzuq (16,945,391 $J \cdot m^{-2} \cdot day^{-1}$), Awbari (15,262,444 $J \cdot m^{-2} \cdot day^{-1}$), Gat (15,106,469 $J \cdot m^{-2} \cdot day^{-1}$), and Awjilah (15,025,188 $J \cdot m^{-2} \cdot day^{-1}$), show high annular beam radiation levels, indicating clear skies, low humidity, and low pollution, or high altitudes.

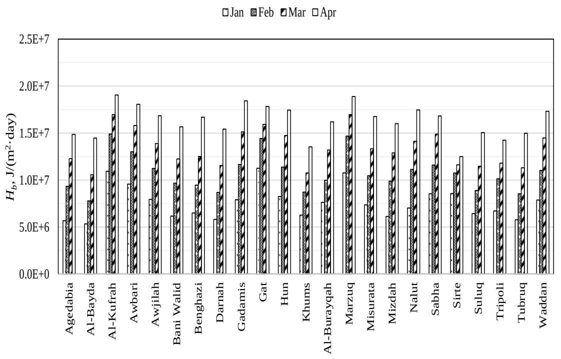

Figure 10. Monthly average daily beam (direct) radiation on a horizontal surface (Jan – Apr).

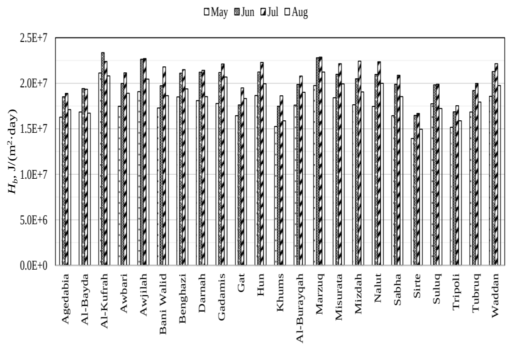

Figure 11. Monthly average daily beam (direct) radiation on a horizontal surface (May – Aug).

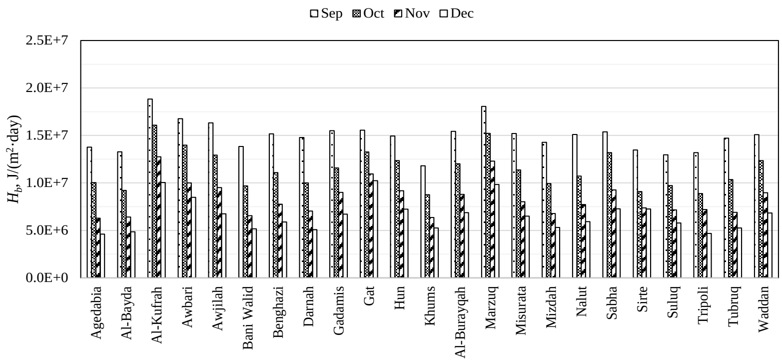

Figure 12. Monthly average daily beam (direct) radiation on a horizontal surface (Sep – Dec)

3.8 Estimation of the ratio of the monthly average daily beam radiation on a tilted surface to that on a horizontal surface

The data in Figures 13, 14, and 15 present the monthly average daily beam radiation on a tilted surface compared to that on a horizontal surface for the months from January to December. As can be seen from the figures, the ratio varies throughout the year due to changes in solar elevation and declination. Benghazi, for example, has a minimum ratio of 0.808 in June and a maximum ratio of 1.858 in December. In general, some locations such as Darnah (1.270), Al-Bayda (1.269), Tripoli (1.268), Khums (1.267), and Misurata (1.263) possess a high annual ratio, indicating that the tilted surface receives more radiation compared to a horizontal surface. Other locations such as Al-Kufrah (1.132), Gat (1.142), Marzuq (1.155), Awbari (1.164), and Sabha (1.171) show a low annual ratio, indicating that the tilted surface receives less radiation compared to a horizontal surface.

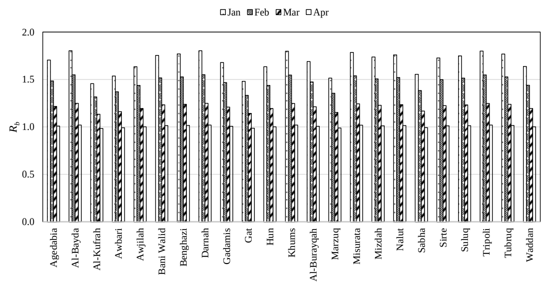

Figure 13. Monthly average daily beam radiation (Jan – Apr).

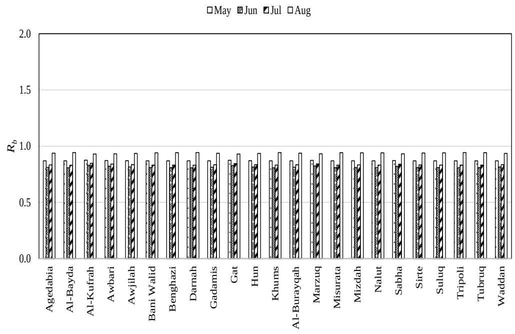

Figure 14. Monthly average daily beam radiation on a tilted surface to that on a horizontal surface (May – Aug).

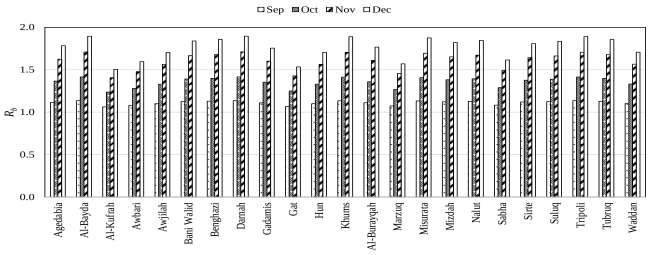

Figure 15. Monthly average daily beam radiation on a tilted surface to that on a horizontal surface (Sep – Dec).

3.9 Estimation of the monthly average daily solar radiation on tilted surface

The data in Figures 16, 17, and 18 present the monthly average daily solar radiation on tilted surfaces from January to December. The solar radiation on a tilted surface changes throughout the year due to the variation in the sun's position in the sky. This variation affects both the angle and intensity of solar radiation received on a tilted surface. The highest estimated monthly average is in Marzuq (26,226,636 $J \cdot m^{-2} \cdot day^{-1}$) for the month of August, and the lowest is in Gat at 19,683,450 $J \cdot m^{-2} \cdot day^{-1}$ for the month of December. Some locations such as Khums (19,097,772 $J \cdot m^{-2} \cdot day^{-1}$), Al-Bayda (19,327,052 $J \cdot m^{-2} \cdot day^{-1}$), Tripoli (19,547,572 $J \cdot m^{-2} \cdot day^{-1}$), Agedabia (19,603,789 $J \cdot m^{-2} \cdot day^{-1}$), and Sirte (19,830,731 $J \cdot m^{-2} \cdot day^{-1}$), show low annual average daily solar radiation on tilted surface. Low solar radiation on a tilted surface means that the surface is receiving a relatively low direct sunlight, resulting in a lower energy production. Other locations such as Al-Kufrah (24,256,829 $J \cdot m^{-2} \cdot day^{-1}$), Marzuq (24,128,866 $J \cdot m^{-2} \cdot day^{-1}$), Gat (22,698,253 $J \cdot m^{-2} \cdot day^{-1}$), Awbari (22,669,531 $J \cdot m^{-2} \cdot day^{-1}$), and Awjilah (22,258,647 $J \cdot m^{-2} \cdot day^{-1}$), show high annual average daily solar radiation on tilted surface. High solar radiation on a tilted surface means that the surface is receiving a significant amount of direct solar energy due to its orientation and angle, resulting in a higher energy production.

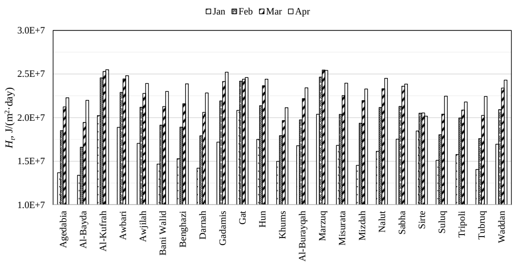

Figure 16. Monthly average daily solar radiation on tilted surface (Jan – Apr)

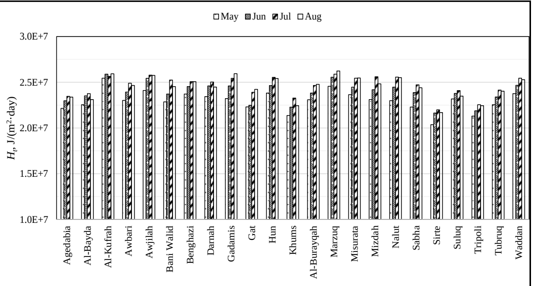

Figure 17. Monthly average daily solar radiation on tilted surface (May – Aug).

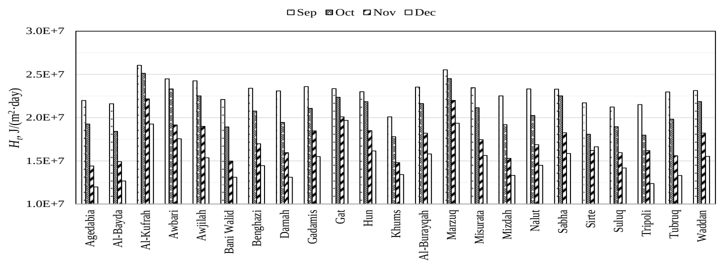

Figure 18. Monthly average daily solar radiation on tilted surface (Sep – Dec).

3.10 Overall analysis

The analysis of the dataset of solar radiation on tilted surfaces for various locations in Libya is shown in Table 2. The mean provides a measure of the central tendency of solar radiation. The median offers an alternative measure of central tendency that is less affected by outliers. The minimum and maximum values delineate the range of the solar radiation measurements, indicating the extent of variability between the smallest and largest values. The standard deviations range from about 19,600,000 $J{\cdot}m^{-2}{\cdot}day^{-1}$ for Agedabia to 25,290,000 $J{\cdot}m^{-2}{\cdot}day^{-1}$ for Al-Kufrah, indicating varying levels of variability in solar radiation measurements. Locations such as Gat and Marzuq demonstrate very low standard deviation values, suggesting consistent solar radiation levels, which is favorable for predictive energy planning. Conversely, a higher standard deviation suggests greater variability. For example, Al-Bayda shows a standard deviation of about 19,449,638 $J{\cdot}m^{-2}{\cdot}day^{-1}$, which reflects that its radiation values may fluctuate significantly within that period. Together, these statistical measures offer a comprehensive understanding of the solar radiation's central tendency, variability, and overall distribution, which is crucial for applications in energy management and environmental studies. Generally, the highest solar radiation values are observed during the summer months, from June to August, especially in Marzuq and Al-Kufrah, indicating optimal conditions for solar energy production during this time. The months of January through March show relatively lower peak values. August stands out as the peak month for solar energy potential, representing an important period for solar energy generation planning.

Table 2. Analysis of monthly mean solar radiation on tilted surfaces for various locations.

Location	Mean	Median	Max	Min	Standard Deviation
	$J \cdot m^{-2} \cdot day^{-1}$	$J \cdot m^{-2} \cdot day^{-1}$	$J \cdot m^{-2} \cdot day^{-1}$	$J \cdot m^{-2} \cdot day^{-1}$	$J \cdot m^{-2} \cdot day^{-1}$
Agedabia	19,603,789	21,228,803	23,459,472	11,972,171	21,228,803
Al-Bayda	19,327,052	19,449,638	23,745,254	12,672,085	19,449,638
Al-Burayqah	21,470,053	22,180,981	24,776,613	15,806,043	22,180,981
Al-Kufrah	24,256,829	25,292,919	26,056,504	19,260,933	25,292,919
Awbari	22,669,532	23,323,790	24,888,592	17,556,639	23,323,790
Awjilah	22,258,647	22,773,351	25,769,703	15,359,966	22,773,351
Bani Walid	20,294,509	21,271,788	25,242,051	13,109,154	21,271,788
Benghazi	21,135,235	21,585,715	25,068,338	14,448,966	21,585,715
Darnah	20,389,464	20,593,627	25,020,267	13,105,378	20,593,627
Gadamis	22,188,204	23,214,250	25,939,738	15,489,406	23,214,250
Gat	22,698,253	22,698,253	24,593,205	19,683,451	22,698,253
Hun	22,151,577	23,004,247	25,535,992	16,152,595	23,004,247
Khums	19,097,772	19,665,789	23,269,752	13,416,071	19,665,789
Marzuq	24,128,866	24,650,601	26,226,636	19,359,014	24,650,601
Misurata	21,698,962	22,530,462	25,471,290	15,619,141	22,530,462
Mizdah	20,596,032	21,950,910	25,600,212	13,315,822	21,950,910
Nalut	21,547,724	22,985,008	25,563,234	14,488,537	22,985,008
Sabha	21,788,289	22,522,258	24,723,089	15,846,738	22,522,258
Sirte	19,830,731	20,359,101	21,982,805	16,203,429	20,359,101
Suluq	20,069,648	20,402,147	24,092,089	14,181,620	20,402,147
Tripoli	19,547,572	20,864,860	22,550,625	12,363,376	20,864,860
Tubruq	20,011,628	20,253,217	24,143,591	13,307,601	20,253,217
Waddan	21,952,376	23,137,001	25,446,928	15,516,943	23,137,001

- *Location-by-location analysis of solar radiation on tilted surface*

The top five locations by mean solar radiation are: Al-Kufrah (24,256,829 $J \cdot m^{-2} \cdot day^{-1}$), Marzuq (24,128,866 $J \cdot m^{-2} \cdot day^{-1}$), Gat (22,698,253 $J \cdot m^{-2} \cdot day^{-1}$), Awbari (22,669,531 $J \cdot m^{-2} \cdot day^{-1}$), and Awjilah (22,258,647 $J \cdot m^{-2} \cdot day^{-1}$). These high-value locations could be less obscured by geographical features such as hills or urban structures, allowing for more direct sunlight exposure throughout the day. In summary, the higher solar radiation values suggest these areas could achieve better electricity generation through solar energy systems, making them prime candidates for solar energy generation projects. The bottom five locations by mean solar radiation are: Khums (19,097,772 $J \cdot m^{-2} \cdot day^{-1}$), Al-Bayda (19,327,052 $J \cdot m^{-2} \cdot day^{-1}$), Tripoli (19,547,572 $J \cdot m^{-2} \cdot day^{-1}$), Agedabia (19,603,789 $J \cdot m^{-2} \cdot day^{-1}$), and Sirte (19,830,731 $J \cdot m^{-2} \cdot day^{-1}$), indicating that they may be the least favorable candidates for solar energy investments. While these locations still have solar potential, they may be less optimal compared to those in the higher group. Environmental factors may limit solar exposure in these areas, such as increased cloud cover, pollution, or geographical obstructions. Although these locations could still produce solar energy, the return on investment might be lower compared to sites in the high group.

4. Discussion and interpretation

4.1 Validation of the model

Validation is the process of assessing whether the model accurately represents the real-world system it is intended to simulate. In this study, the estimated solar radiation data are compared to the global horizontal irradiance (GHI), Figure 19. The comparison will aid in understanding how well the measured or estimated solar radiation data aligns with this benchmark. The results shown in Table 3 show that estimated solar radiation data are generally in agreement with the GHI. Overall, the results suggest that the estimated solar radiation data are generally reliable and can be used as a basis for further analysis.

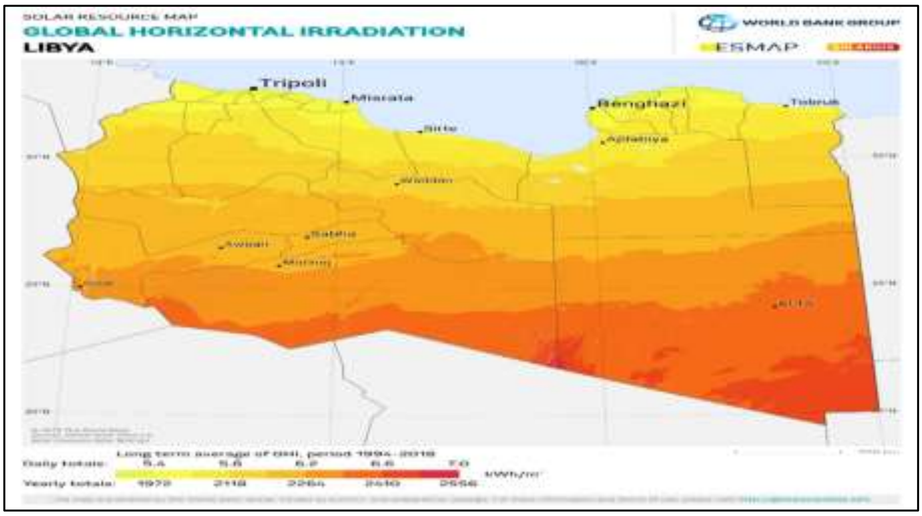

Figure 19. Daily total GHI for Libya (Free Maps & GIS Data Solargis 2023).

Table 3. Comparison of estimated the estimated solar radiation to the GHI, kWh·m^{-2}·day^{-1}.

Location	Estimated mean solar radiation	GHI (Center, 2024)	Comparison with GHI	Analysis
Agedabia	5.4	5.7	Lower by 0.3	Slightly below average; potential to improve solar capture
Al-Bayda	5.4	5.5	Lower by 0.1	Close to GHI; stable energy conditions likely
Al-Kufrah	6.7	6.7	Equal	Excellent solar potential; very consistent
Awbari	6.3	6.4	Lower by 0.1	Good solar performance; marginal improvement possible.
Awjilah	6.2	5.9	Higher by 0.3	Strong solar potential; suitable for energy projects.
Bani Walid	5.6	5.7	Lower by 0.1	Reliable, but slight room for growth exists
Benghazi	5.9	5.6	Higher by 0.3	Strong solar potential; suitable for energy projects.
Darnah	5.7	5.5	Higher by 0.2	Positive outlook; solid solar energy generation.
Gadamis	6.2	5.9	Higher by 0.3	Strong solar potential; suitable for energy projects.
Gat	6.3	6.4	Lower by 0.1	Competitive solar capacity
Hun	6.2	5.9	Higher by 0.3	Strong solar potential; suitable for energy projects.
Khums	5.3	5.6	Lower by 0.3	Below average; requires exploration of enhancing measures.
Al-Burayqah	6.0	5.7	Higher by 0.3	Strong solar potential; suitable for energy projects.
Marzuq	6.7	6.2	Higher by 0.5	Exceptional potential; optimal conditions for solar projects.
Misurata	6.0	5.6	Higher by 0.4	Good performance; promising for solar investments.
Mizdah	5.7	5.7	Equal	Efficient energy generation; stable solar resource.
Nalut	6.0	5.7	Higher by 0.3	Strong solar potential; suitable for energy projects.
Sabha	6.1	6.2	Lower by 0.1	Close to ideal; competitive landscape for resources.
Sirte	5.5	5.7	Lower by 0.2	Moderate performance; room to improve solar efficiency.
Suluq	5.6	5.7	Lower by 0.1	Average solar performance; potential for upgrades exists.
Tripoli	5.4	5.5	Lower by 0.1	Slightly below average
Tubruq	5.6	5.6	Equal	Consistent performance; predictable energy generation.
Waddan	6.1	5.9	Higher by 0.2	Good potential; suitable for solar energy projects.

The highest estimated mean solar radiation is observed in Al-Kufrah, Marzuq, Gat, Awbari, Awjilah, Gadamis, Hun, Waddan, Sabha, Misurata, and Nalut in order, while the lowest estimated mean solar radiation is observed in: Khums, Al-Bayda, Tripoli, Agedabia, Sirte, Tuburq, Suluq, Bani Walid, Darnah, Mizdah, Benghazi, and Al-Burayqah. The difference between the estimated and the GHI values indicates potential issues with GHI measurements or due to environmental factors such as shading, and atmospheric conditions. The difference could also suggest solar radiation was either underreported, or the measurement conditions for GHI were more favorable. In three locations Al-Kufrah, Mizdah, and Tuburq, GHI matches the estimated mean solar radiation, indicating a reliable and consistent assessment of solar potential. In conclusion, understanding the discrepancies between estimated mean solar radiation and GHI could guide future solar energy projects and investments in these areas.

To provide a more comprehensive understanding of the solar energy potential in Libya, the results of this study are compared to similar studies and projects in the region of similar climatic conditions. This comparison will help to identify areas of consistency and variation, and provide a more nuanced understanding of the solar energy potential in Libya. A study conducted in Egypt (Salah et al., 2022) found that the country's solar radiation values range from 2,100 to 2,400 $kWh \cdot m^{-2}$ per year, with the highest values observed in the western desert region. Tunisia's solar radiation values range from 1,900 to 2,400 $kWh \cdot m^{-2}$ per year, with the highest values occurring in the northern and central regions (Othman et al., 2018). Morocco reports values between 1,800 and 2,300 $kWh \cdot m^{-2}$ per year, with the highest values in the southern regions (El Mghouchi et al., 2016). In comparison, Libya generally exhibits higher average solar radiation levels than Tunisia and Morocco. Studies conducted in desert climates such as Algeria, Chad, and Mali have reported similar solar radiation levels to those found in Libya. For example, Algeria reports values ranging from 2,000 to 3,000 $kWh \cdot m^{-2}$ per year (Aoun & Bouchouicha, 2017). The Sahel region, which spans across Africa from Senegal to Ethiopia demonstrates similar solar potential, with radiation values between 1,800 to 2,500 $kWh \cdot m^{-2}$ per year in Niger, for example (Niang et al., 2023).

4.2 Implications and significance of the study results

The information emphasizes how solar energy could help enhance Libya's renewable energy options, aiding in the country's shift toward a greener economy. This data can help shape policy choices on renewable energy goals, grid connection, and investment motivations. The estimated data on solar radiation offers detailed insights into the solar energy potential of various regions, allowing developers to pinpoint appropriate sites for solar projects, enhance system design and reduce expenses.

4.3 Identification of key findings and trends related to solar energy potential

The study indicates that Libya has significant potential for solar energy, with estimated solar radiation values ranging from 1,936 $kWh \cdot m^{-2}$ for Khums to 2,459 $kWh \cdot m^{-2}$ per year for Al-Kufrah. The study also shows a general trend of increasing solar radiation values as one moves towards the southern regions. The data also indicates that solar radiation values vary seasonally, with peak values typically occurring during the summer months. The mountainous regions, however, tend to have lower solar radiation values due to the shading effect of the mountains and reduced sunlight penetration.

5. Conclusion

To conclude, this study presents and evaluates the estimation of solar radiation for various locations in Libya based on the fundamental principles of physics and meteorology. Real data were used as an input to the model. The study categorizes the locations into high-solar and low-solar radiation groups. The high-solar radiation regions, including Al-Kufrah, Marzuq, and Gat, show significantly elevated solar radiation levels, making them particularly favorable for solar energy investments. In contrast, the low-solar radiation group, including Khums and Al-Bayda, shows reduced solar energy potential, which may impact the economic viability of solar projects in these locations. The comparison of estimated solar radiation data with GHI benchmarks indicates generally reliable measurements, though some discrepancies suggest potential issues with GHI data accuracy or environmental factors affecting solar exposure. This study’s findings can guide strategic decisions for solar energy development, optimize system designs, maximize investment returns, and better planning and implementation of solar projects. Overall, Libya's substantial solar energy potential positions the country as a promising candidate for expanding renewable energy initiatives and contributing to the global transition to sustainable energy. This study, however, can be enhanced by incorporating detailed geographical surveys, including topography and land use, as well as further study on albedo and local ground measurements.

References

Almaktar, M., & Shaaban, M. (2021). Prospects of renewable energy as a non-rivalry energy alternative in Libya. *Renewable and Sustainable Energy Reviews*, *143*, 110852.

Aoun, N., & Bouchouicha, K. (2017). Estimating daily global solar radiation by day of the year in Algeria. *The European Physical Journal Plus*, *132*, 1-12.

Atmospheric Science Data Center. [Accessed June 20th. (2020). *Processing, archiving and distributing Earth science data at the NASA Langley ResearchCenter. [Online] Available from: https://eosweb.larc.nasa.gov/*

Center, A. S. D. C. R. (2024). *Processing, archiving and distributing Earth science data at the NASA Langley*

Chandler, W. S., Whitlock, C. H., & Stackhouse Jr, P. W. (2004). NASA climatological data for renewable energy assessment. *J. Sol. Energy Eng.*, *126*(3), 945-949.

Cooper, P. (1969). The absorption of radiation in solar stills. *Solar energy*, *12*(3), 333-346.

Duffie, J. A., & Beckman, W. A. (1980). *Solar engineering of thermal processes*. Wiley New York.

Eicker, U. (2003). *Solar technologies for buildings*. John Wiley & Sons.

El Mghouchi, Y., Ajzoul, T., & El Bouardi, A. (2016). Prediction of daily solar radiation intensity by day of the year in twenty-four cities of Morocco. *Renewable and Sustainable Energy Reviews*, *53*, 823-831.

Erbs, D., Klein, S., & Duffie, J. (1982). Estimation of the diffuse radiation fraction for hourly, daily and monthly-average global radiation. *Solar energy*, *28*(4), 293-302.

Free Maps & GIS Data Solargis (2023). .https://solargis.com/resources/free-maps-and-gis-data?locality=libya,

Iqbal, M. (2012). *An introduction to solar radiation*. Elsevier.

Irhiam, H., Schaeffer, M., & Watanabe, K. (2023). *The Long Road to Inclusive Institutions in Libya: A Sourcebook of Challenges and Needs*. World Bank Publications.

Liu, B. Y., & Jordan, R. C. (1960). The interrelationship and characteristic distribution of direct, diffuse and total solar radiation. *Solar energy*, *4*(3), 1-19.

Majeed, Y., Khan, M. U., Waseem, M., Zahid, U., Mahmood, F., Majeed, F., Sultan, M., & Raza, A. (2023). Renewable energy as an alternative source for energy management in agriculture. *Energy Reports*, *10*, 344-359.

Matori, S. S. (2024). *Energy transition and climate-related policies: A changing environment and its implications for OPEC countries* Technische Universität Wien].

Mohamed, O. A., & Masood, S. H. (2018). A brief overview of solar and wind energy in Libya: Current trends and the future development. IOP Conference Series: Materials Science and Engineering,

Niang, S. A. A., Gueye, A., Sarr, A., Diop, D., Goni, S., & Nebon, B. (2023). Comparative Study of Available Solar Potential for Six Stations of Sahel. *Smart Grid and Renewable Energy*, *14*(8), 153-167.

Othman, A. B., Belkilani, K., & Besbes, M. (2018). Global solar radiation on tilted surfaces in Tunisia: Measurement, estimation and gained energy assessments. *Energy Reports*, *4*, 101-109.

Prescott, J. (1940). Evaporation from a water surface in relation to solar radiation. *Trans. Roy. Soc. S. Aust.*, *46*, 114-118.

Ritchie, H., Rosado, P., & Roser, M. (2024). Access to energy. *Our World in Data*.

Salah, S. I., Eltaweel, M., & Abeykoon, C. (2022). Towards a sustainable energy future for Egypt: A systematic review of renewable energy sources, technologies, challenges, and recommendations. *Cleaner Engineering and Technology*, *8*, 100497.

Stephens, G. L., O'Brien, D., Webster, P. J., Pilewski, P., Kato, S., & Li, J. l. (2015). The albedo of Earth. *Reviews of geophysics*, *53*(1), 141-163.

Strielkowski, W., Civín, L., Tarkhanova, E., Tvaronavičienė, M., & Petrenko, Y. (2021). Renewable energy in the sustainable development of electrical power sector: A review. *Energies*, *14*(24), 8240.

Yadav, P., Davies, P. J., & Sarkodie, S. A. (2019). The prospects of decentralised solar energy home systems in rural communities: User experience, determinants, and impact of free solar power on the energy poverty cycle. *Energy Strategy Reviews*, *26*, 100424.

Yahya, W., Nassar, A., Mansur, F. A., Al-Nehari, M., & Alnakhlani, M. (2020). Future study of renewable energy in Libya. *International Journal of Advanced Engineering Research and Science (IJAERS)*, *7*(10), 1-6.

مستقبل الطاقة المستدامة في ليبيا:
تقييم إمكانات الطاقة الشمسية في ثلاث وعشرين منطقة حضرية

جمعة النعاس[1] ,عبدالسلام الشريف[1] , محمد التريكي[2]

[1]قسم الهندسة الكيميائية والنفط ، كلية الهندسة الخمس، جامعة المرقب، ليبيا

E-mail: alnaasjumaa@gmail.com, a6sharif@uwaterloo.ca

[2]المركز الليبي لأبحاث التنمية المستدامة، الهيئة الليبية للبحث العلمي، ليبيا

E-mail: mstraiki@lsd.ly

المستخلص

إمكانات الطاقة الشمسية في ليبيا هائلة وغير مستغلة إلى حد كبير. من خلال استغلال هذه الموارد بشكل استراتيجي، يمكن لليبيا أن تتقدم نحو مستقبل مستدام في مجال الطاقة يقلل من اعتمادها على الوقود الأحفوري، ويخفض انبعاثات الكربون، ويعزز النمو الاقتصادي. تقوم هذه الدراسة بتقييم إمكانات الطاقة الشمسية في ليبيا من خلال تحليل بيانات الإشعاع الشمسي في ثلاث وعشرين مدينة في جميع أنحاء البلاد باستخدام بيانات من قاعدة بيانات ناسا. تشير الدراسة إلى أن ليبيا مؤهلة بدرجة عالية للطاقة الشمسية، حيث تظهر مختلف المناطق قيم إشعاع شمسي مقدرة تتراوح بين 1936 كيلوواط ساعة/م^2 للخمس و2459 كيلوواط ساعة/م^2 في السنة للكفرة. تُظهر المناطق الجنوبية، ولا سيما الكُفرة 24,256,829 جول/م^2 لليوم، مرزق 24,128,866 جول/م^2 لليوم، وغات 22,698,253 جول/م^2 لليوم، أعلى مستويات الإشعاع الشمسي، مما يجعلها مرشحة رئيسية لمشاريع الطاقة الشمسية على نطاق واسع. بالمقابل، تُظهر المدن الشمالية إشعاعًا شمسيًا أقل بالمقارنة مثل الخُمس 19,097,772 جول/م^2 لليوم، البيضاء 19,327,052 جول/م^2 لليوم، وطرابلس 19,547,572 جول/م^2 لليوم، مما يشير إلى جدوى أقل لتركيب نظم الطاقة الشمسية. تظهر التغيرات الموسمية، خاصة خلال فصل الصيف، إمكانية قصوى للطاقة الشمسية، مما يؤكد على الحاجة إلى التخطيط الاستراتيجي وإمكانية دمج حلول تخزين الطاقة. تتوافق نتائج الدراسة مع الاتجاهات الإقليمية للإشعاع الشمسي الملاحظة في مناخات مماثلة، مما يثبت دقة النموذج المستخدم. تقدم هذه الدراسة رؤى هامة لصانعي السياسات والمستثمرين، مما يدعم انتقال ليبيا نحو الطاقة المتجددة ويسهم في تحقيق أهداف الاستدامة الخاصة بها.

الكلمات المفتاحية: الطاقة الشمسية، الإشعاع الشمسي، الطاقة المتجددة، ليبيا.